

Ultrasound-Mediated Drug Delivery and Gene Therapy

Subjects: [Cell Biology](#) | [Oncology](#)

Contributor: Candace M. Howard

Ultrasound (US) is a nearly innocuous and widely available imaging technique with a well-established role in various diagnostic applications. Diagnostic US techniques use high frequency ultrasound waves to view real-time tissue and organs inside the human body. The use of US as a drug delivery facilitator was first described in the mid 90s, using the physical transient increased cell membrane permeability from sonoporation. Subsequent research reported the enhanced biophysical effects of ultrasound by incorporation of MBs.

Ultrasound

cancer

Gene delivery

1. MBs Mechanics and Ultrasound Technique

Ultrasound (US) is a nearly innocuous and widely available imaging technique with a well-established role in various diagnostic applications. Diagnostic US techniques use high frequency ultrasound waves to view real-time tissue and organs inside the human body. The use of US as a drug delivery facilitator was first described in the mid 90s, using the physical transient increased cell membrane permeability from sonoporation [\[1\]](#)[\[2\]](#)[\[3\]](#). Subsequent research reported the enhanced biophysical effects of ultrasound by incorporation of MBs [\[4\]](#)[\[5\]](#).

The use of MBs as ultrasound contrast enhancement agents has dramatically evolved in recent years, particularly after the US Food and Drug Administration (FDA) first approval for use in clinical practice in 2001. MBs are gas-filled spherical voids coated by a stabilizing shell composed of phospholipids, proteins, or synthetic polymer materials, measuring approximately 1–10 μm . The difference between the acoustic impedance of the MBs' gas filling composition (e.g., perfluorocarbon, sulfur hexafluoride, or nitrogen) and the surrounding blood is highly reflective and generates an enhanced acoustic backscattering from blood [\[6\]](#).

In clinical practice, diagnostic US takes advantage of the physical properties of MBs made possible by its resonance behavior. Under the compressibility variations of US waves along with the surrounding liquid inertia, MBs respond with a mass-spring-like resonance behavior whose frequency obeys an inverse relation with the bubble radius [\[7\]](#). Thus, at routinely diagnostic low acoustic powers, MBs compressibility mainly generates synchronous oscillations and linear echo emissions, which provides contrast enhancement commonly used in assessment of cardiac function and characterization of visceral lesions in diagnostic imaging [\[8\]](#).

However, under effects near its resonance frequency, the bubble displays maximal radial response and generates secondary effects, such as harmonics and subharmonics, microstreaming, acoustic radiation forces, shape

instabilities, and non-spherical oscillations [7]. These effects have been previously described in clinical applications such as non-invasive vascular pressure estimation [8], bacterial biofilms removal [9], mechanical destruction of thrombus or tumors [10], or vessel wall permeability induction [11].

Given MBs' compressible core, they are able to respond to ultrasound pressure wave oscillations, a process known as cavitation. Thus, cavitation of MBs varies according to resonance frequency, pulse repetition frequency, acoustic power, gas core composition, damping coefficients, and shell properties [12]. Since acoustic power is the most important US parameter to determine MBs' response, it further divides the cavitation process into stable, when low acoustic pressure ultrasound is applied, or inertial, when high acoustic pressures are applied.

The cavitation process at low acoustic pressures is called stable, because the net of influx and efflux of gas during MBs' compressibility and expansion phases is zero. At high acoustic pressures, however, the expansion phase is extended and MBs oscillate in a non-linear fashion.

Furthermore, when expansion reaches its resonant size, MBs oscillate in a low amplitude, creating microstreams of blood flow around them [13]. Coupled with microstreams, the ultrasound acoustic radiance force generates displacement of fluid and particles in the direction of the sound wave propagation driven by the radiance force from scatters and reflectors in the ultrasound field, a process known as bulk stream. The bulk stream is important in gene therapy applications, since distance between MBs and the target cell membrane has been observed to influence the degree of pore formation in previous studies [14][15]. The intensity of the bulk and micro streams is dependent on the applied US parameters, and when in proximity to the blood vessel wall, is able to produce shear stress, inducing pore formation [16][17][18]. Importantly, the biological effects of the microstreaming production vary drastically according to the acoustic pressure setting. Specifically, at lower acoustic pressures MBs micro shearing induces rapidly reversible pore formation; while at higher acoustic pressures, pore formation may be followed by cell death. Each setting may be applicable in different clinical scenarios. For instance, the reversible pore formation has been used to safely transpose membranes and target drug and gene therapy to diseased tissue. On the other hand, higher acoustic pressures have been used when tissue death is desirable such as oncologic applications [11].

Previous studies hypothesized that the cavitation process in MBs interacts with the cell membrane integrity by generation of a push and pulling effect. Multiple authors studied the impact of different levels of acoustic pressure on the cellular membrane deformation. Experimental studies demonstrated a high correlation between acoustic pressure level and cellular membrane deformation. Wang et al. also studied the impact of bubble-to-cell distance and their interaction using a boundary element method model. The authors found that the degree of cell membrane deformation inversely correlated with widening of the bubble–cell membrane gap [19].

Besides the effect of acoustic radiation force, another potentially useful approach to reduce the bubble-to-cell membrane distance is the use of targeted MBs. Kooiman et al. investigated the influence of microbubble targeting in sonoporation effectiveness and reported that targeted MBs are able to induce pore formation at peak negative pressures 2–5 times lower compared to non-targeted MBs [20].

A second mechanism used by the ultrasound microbubble system for enhanced targeted therapy delivery is microjet formation. Once the extended expansion generated by high acoustic pressure leads to MBs collapse, a membrane disruption may be produced resulting in microjet formation. The microjets are generally oriented towards the shock wave propagation direction; however, when in proximity to highly reflective tissues, the direction of the microjet may be less predictable [21]. Endothelial cell membrane pore formation by shear stress generated by microstreams and microjet formation are the main mechanisms utilized to enhance tumor drug delivery, since it allows for increased localized vessel permeability. **Figure 1** illustrates the biophysical effects of ultrasound on MBs.

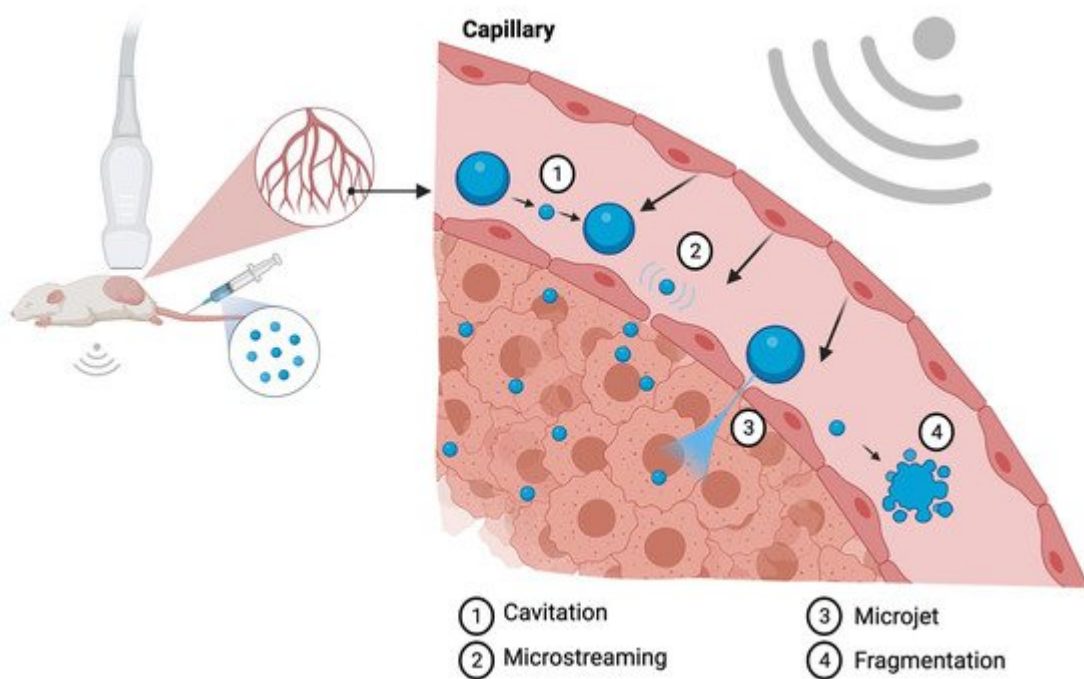


Figure 1. Illustration of the biologic effects of MBs sonification at the capillary level. The cavitation process (1) represents the change in MB diameter reflecting in expansion and shrinking resultant of acoustic pressure variation. Microstreaming (2) is regarded as one of the major biological effects able to induce pore formation through a process of microshearing. Microjet formation (3) and fragmentation (4) are the mechanisms observed at the maximal expansion phase of the cavitation process. Created with [BioRender.com](#).

Another important ultrasound parameter reported to modify cell membrane response to microbubble cavitation is pulse length. It is known that MBs move toward each other as a consequence of secondary acoustic radiation forces, which is increased by longer pulse lengths, and that increases aggregation rate, reducing delivery effectiveness. Experimental studies investigated the microbubble behavior at two different wave lengths: 10 ms and 10 μ s, maintaining acoustic pressure at 400 kPa. The authors observed high delivery rates and higher cell viability with short pulse length and massive cell death with low delivery rates at longer pulse length [22]. Thus, although most studies using sonoporation to enhance therapy delivery employ long pulse lengths, the use of shorter pulse lengths may also be employed to aid in therapy delivery rates, avoid MBs aggregation and related deleterious outcomes to surrounding normal tissue [23].

The biological effects of microbubble sonoporation on the cell membrane are of particular interest to theragnostic research. Wang et al. demonstrated that sonoporation induces disruption of the cytoskeleton, in particular the alfa-tubulin arrangement, and enhances permeability of the cell membrane to MBs, a process that highly correlates with acoustic power. Furthermore, Wang et al. demonstrated that in the intracellular delivery facilitated by sonoporation, the enhancement rate of membrane permeability correlates with the disassembly of the cytoskeleton network [24][25][26].

2. Alternative Formulations

Despite the advantageous biological effects generated by MBs' sonoporation, extensive research has been employed to improve its penetration into the vessel walls, for which the bubble size continues to confer a limitation. The normal endothelial tissue is able to permit diffusion of particles between about 380 and 780 nm, which limits MBs passive diffusion. Thus, the use of nanobubbles (NBs) has also been extensively studied in recent years in an effort to overcome particle size challenges and enhance drug delivery. Similar to MBs, NBs are composed of different shell and core materials and may be coupled with specific tissue ligands for targeted tissue delivery. Several studies have demonstrated the higher passive extravasation rate of NBs compared with micron-sized bubbles. These smaller contrast agents are capable of penetrating tissues more easily and preferably by passive intact extravasation, a potential advantage to therapeutic and diagnostic applications that has been extensively explored in preclinical studies [27]. These characteristics may pose a set of advantages over micron-sized bubbles such as deeper therapeutic delivery potential in NBs-loaded and diagnostic when NBs are tagged. Although initially contrast enhancement was a concern with the use of NBs, recently, phospholipid-shell formulations have demonstrated better ultrasound enhancement performance. Moreover, a higher retention time was demonstrated once tagged NBs arrived at the target tissue given its higher extravascular permeability. Sonification of the tissue of interest tends to generate coalescence of NBs into MBs, which increases its acoustic radiance enhancement properties [28].

Despite its advantages, NBs preparation still poses several challenges to its clinical application. These include the need for centrifugation prior to injection, a higher rate of impurities caused by byproducts, and the need of amphilic surfactants [29]. Initial reports demonstrated concern with NBs regarding their much lower echogenicity in ultrasound imaging compared to MBs [29][30]. Furthermore, due to the typical disorganized intra-tumoral vascular structure and consequent reduced internal blood flow, NBs' distribution may become limited beyond the vascular endothelial wall, and there is a concern with interpretation of a potential uneven response. Despite its preclinical excitement, clinical studies using NBs have not been so fruitful, a disparity probably explained by the heterogeneity of tumoral microenvironment that influences NBs distribution and response.

Droplets and nanodroplets, also known as pulse-change emulsions, encompass a recent new category of cavitation particles being studied for diagnostic and therapeutic interventions. Liquid emulsion in droplets arose from the need for more stable cavitation agents with longer blood-half-life than MBs, since the liquid core prevents gas dissolution. Oil emulsions stabilized by surfactant coating are already in use in different clinical applications, such as aerosols and penicillin droplets. Droplets have also found use in a variety of diagnostic applications

including fluorine-19 magnetic resonance imaging [31], positron emission tomography [32], and ultrasound [33] imaging. The development of triggered and controlled release of therapeutic payload was explored with the use of superheated core such as perfluorocarbons. The superheated core droplets are able to remain stable until exposed to an external stimulus, such as focused ultrasound, whereby liquid-to-gas transition takes place. After sonification, the nano-droplet vaporizes into a gas bubble in the target tissue and becomes susceptible to the same cavitation changes described for MBs earlier. The main advantages of the superheated core nano-droplet technology are the possibility of increased acoustic emissions and harmonic content in the target tissue, with longer circulation time and cell membrane diffusion capability [31][32][33].

Although promising, the use of droplets in clinical oncologic applications still has several challenges to overcome. Since the efficacy of ultrasound enhancement and tumor targeting of droplets largely depend on shell and perfluorocarbon core composition, studies are still needed to define the best materials for clinical application. The ideal threshold of vaporization while maintaining thermal stability demands a definition of a material that will remain stable at physiological temperatures and transition into a microbubble at a low vaporization threshold without damaging the surrounding normal tissue [34]. The first generation of droplets liquid emulsion is using perfluorocarbon.

3. Types of Shell Composition

There are two general types of bubbles known to be responsive to the sonoporation application: free bubbles and encapsulated bubbles. Free bubbles are simply cavities filled with air or other gases while encapsulated MBs consist of cavities surrounded by a capsule of variable composition. **Table 1** summarizes types of carriers and their properties.

The sonoporation clinical application was first studied using free bubbles. The physical dynamics of free bubbles are described by the Rayleigh–Plesset equation and will produce, essentially, the same biophysical effects described earlier characterized by sonoporation. However, unlike encapsulated MBs, free bubbles have no boundaries, and under the biophysical effects of ultrasound, compression and decompression leads to instability and effects are poorly predictable [35].

Similar to free bubbles, encapsulated MBs are able to circulate in the blood stream until they reach the area of interest. The biological effects of MBs are highly dependent on the gas core and shell composition and respond differently according to US setting parameters. Over the years, researchers developed numerous strategies to enhance MBs stability and targeting by coating with polymers, proteins, or lipids. The engineering of different combinations of shell and gaseous core also allowed improvement of scattering effect and contrast-to-background tissue ratio [36].

Currently, phospholipid coating is the most used shell composition, since it allows for high biocompatibility, flexibility, and enhanced non-linear properties. Moreover, a phospholipid coating may be further enhanced by the addition of numerous molecules, such as polyethylene glycol (PEG), which reduces interaction with immunologic

cells and allows coupling with targeting ligands, genes, or chemotherapeutics, turning them into potential therapy microcarriers [37].

As mentioned above, the cavitation behavior of MBs varies greatly between different shell compositions given their particular viscoelastic properties. For instance, phospholipidic shells are typically composed of a thinner flexible layer which allows them to oscillate at low acoustic pressures. Once rupture is reached, these lipidic MBs tend to form smaller subsets which surround the main particle. Hard shell MBs, in contrast, typically bear a thicker shell layer and thus require higher acoustic pressures to reach cavitation. Moreover, due to higher acoustic pressure, fragmentation of hard-shelled MBs results in a more aggressive fragmentation known as sonic cracking, capable of propelling the core gas a few microns away [9][38][39]. Liu et al. analyzed molecule delivery efficiency of MBs in 26 studies using different US parameters and shell compositions. The authors noted that a more efficient uptake was associated with the use of Definity contrast agent (lipid shell) compared to Optison (albumin shell) in the analyzed studies [40]. The authors also highlighted the association of temperature with higher uptake efficiency, with better results reported at 37 °C. In an effort to minimize confounding variables from different ultrasound parameters and MBs concentration from the different studies, Liu et al. reproduced an experiment with fixed US parameters and confirmed higher dextran delivery efficiency using Definity contrast agents compared to Optison at 37 or 23 °C.

Table 1. Types of carriers and their properties.

	Mechanism	Cavitation Threshold	Advantages	Limitations	References
Lipid shell	Cavitation, endocytosis	Low	Easy labeling and therapy loading. Low immunogenic profile	Limited loading capacity	[9][32][34]
Albumin shell	Disulfide crosslink formation and fragmentation	High	Simple formulation	Unable to bind negatively charged molecules	[38][39]
Polymer shell	Fragmentation	High	Able to accommodate hydrophobic and hydrophilic molecules	High cavitation threshold may damage surrounding normal tissue	[41]
Nanobubbles	Cavitation and aggregation	Low	Passive endothelial penetration	Low echogenicity impairs contrast and potentially tissue targeting	[27][28][29][30]
Droplets	Pulse-change emulsion	Variable	Increased half-life by avoiding immediate gas dissolution	Narrow cavitation threshold	[31][32][33]
Nanoparticles	Hyperthermia, cavitation, free	Variable	Functionalization	Safety profile, variable and/or	[42]

Mechanism	Cavitation Threshold	Advantages	Limitations	References
radicals			unknown toxicity	nation. In cturing of

the capsule and subsequent release of the gas core. Ultrasound pressure thresholds for sonic cracking are reported between 400 and 1200 kPa, typically higher than the ones needed for lipid-shell cavitation. Induced cell permeability correlates with the extent of sonic cracking allowing effective large pore formation; however, normal tissue and endothelial cell viability remains a concern at higher acoustic power parameters [41].

The simplest way to load albumin-shell MBs is by incubation of viral vectors and drugs of interest. Unfortunately, this strategy is inefficient for coating non-viral gene therapy due to the negative charges on both the protein shell and the nucleic acid backbone. A second mechanism utilized to circumvent this limitation is the gene therapy crosslinking into the protein matrix at its formation stage. This has shown to effectively deliver therapy when sonification is applied by fragmentation [43][44].

4. Kinetics

MBs are isotonic to human plasma and can circulate through capillaries, given their small size. After intravenous injection, MBs dissolve producing remnants that are readily metabolized and cleared, minimizing risk of emboli. The biodistribution and clearance properties vary greatly between different MBs' shell and core compositions with reported half-lives ranging from 1 min for albumin shell and air core to up to 180 min in lipid shell with N2/perfluorohexane core [45]. The short half-life of most commonly used ultrasound contrast agent MBs is caused by their temporary retention in lung, liver, and spleen along with their rapid disintegration in small vessels. The safety profile of MBs is considered good, with rare reported side effects including dizziness, erythematous rash, itching, nausea, vomiting, dyspnea, bronchospasm, hypotension, bradycardia, cutaneous rash, back pain, and clouding of consciousness [46].

References

1. Forsberg, F.; Basude, R.; Liu, J.-B.; Alessandro, J.; Shi, W.T.; Rawool, N.M.; Goldberg, B.B.; Wheatley, M.A. Effect of filling gases on the backscatter from contrast microbubbles: Theory and in vivo measurements. *Ultrasound Med. Biol.* 1999, 25, 1203–1211.
2. Gupta, I.; Eisenbrey, J.R.; Machado, P.; Stanczak, M.; Wessner, C.E.; Shaw, C.M.; Gummadi, S.; Fenkel, J.M.; Tan, A.; Miller, C.; et al. Diagnosing portal hypertension with noninvasive subharmonic pressure estimates from a US contrast agent. *Radiology* 2021, 298, 104–111.
3. Hernot, S.; Klibanov, A.L. Microbubbles in ultrasound-triggered drug and gene delivery. *Adv. Drug Deliv. Rev.* 2008, 60, 1153–1166.

4. Lazzari, C.; Karachaliou, N.; Bulotta, A.; Viganó, M.; Mirabile, A.; Brioschi, E.; Santarpia, M.; Gianni, L.; Rosell, R.; Gregorc, V. Combination of immunotherapy with chemotherapy and radiotherapy in lung cancer: Is this the beginning of the end for cancer? *Ther. Adv. Med. Oncol.* 2018, 10, 1–12.
5. Meairs, S. Sonothrombolysis. *Transl. Neurosonology* 2015, 36, 83–93.
6. Miller, D.L.; Bao, S.; Morris, J.E. Sonoporation of cultured cells in the rotating tube exposure system. *Ultrasound Med. Biol.* 1999, 25, 143–149.
7. Ross, J.P.; Cai, X.; Chiu, J.-F.; Yang, J.; Wu, J. Optical and atomic force microscopic studies on sonoporation. *J. Acoust. Soc. Am.* 2002, 111, 1161–1164.
8. Dollet, B.; van der Meer, S.M.; Garbin, V.; de Jong, N.; Lohse, D.; Versluis, M. Nonspherical oscillations of ultrasound contrast agent microbubbles. *Ultrasound Med. Biol.* 2008, 34, 1465–1473.
9. De Jong, N.; Bouakaz, A.; Frinking, P. Basic acoustic properties of microbubbles. *Echocardiography* 2002, 19, 229–240.
10. Sijl, J.; Dollet, B.; Overvelde, M.; Garbin, V.; Rozendal, T.; De Jong, N.; Lohse, D.; Versluis, M. Subharmonic behavior of phospholipid-coated ultrasound contrast agent microbubbles. *J. Acoust. Soc. Am.* 2010, 128, 3239–3252.
11. Singh, V.; Khan, N.; Jayandharan, G.R. Vector engineering, strategies and targets in cancer gene therapy. *Cancer Gene Ther.* 2021, 1–16.
12. Song, K.-H.; Harvey, B.K.; Borden, M.A. State-of-the-art of microbubble-assisted blood-brain barrier disruption. *Theranostics* 2018, 8, 4393–4408.
13. Ward, M.; Wu, J.; Chiu, J.-F. Ultrasound-induced cell lysis and sonoporation enhanced by contrast agents. *J. Acoust. Soc. Am.* 1999, 105, 2951–2957.
14. Wiklund, M.; Green, R.; Ohlin, M. Acoustofluidics 14: Applications of acoustic streaming in microfluidic devices. *Lab Chip* 2012, 12, 2438–2451.
15. Zhou, Y.; Yang, K.; Cui, J.; Ye, J.; Deng, C. Controlled permeation of cell membrane by single bubble acoustic cavitation. *J. Control. Release* 2012, 157, 103–111.
16. VanBavel, E. Effects of shear stress on endothelial cells: Possible relevance for ultrasound applications. *Prog. Biophys. Mol. Biol.* 2007, 93, 374–383.
17. Xia, Y.; Du, Z.; Wang, X.; Li, X. Treatment of uterine sarcoma with rAd-p53 (Gendicine) followed by chemotherapy: Clinical study of TP53Gene therapy. *Hum. Gene Ther.* 2018, 29, 242–250.
18. Quaia, E. Physical basis and principles of action of microbubble-based contrast agents. In *Contrast Media in Ultrasonography. Medical Radiology (Diagnostic Imaging)*; Quaia, E., Ed.;

Springer: Berlin/Heidelberg, Germany, 2005.

19. Duc, N.M.; Keserci, B. Emerging clinical applications of high-intensity focused ultrasound. *Diagn. Interv. Radiol.* 2019, 25, 398–409.
20. Dunbar, C.E.; High, K.A.; Joung, J.K.; Kohn, D.B.; Ozawa, K.; Sadelain, M. Gene therapy comes of age. *Science* 2018, 359, eaan4672.
21. Wu, J.; Ross, J.P.; Chiu, J.-F. Reparable sonoporation generated by microstreaming. *J. Acoust. Soc. Am.* 2002, 111, 1460–1464.
22. Cheng, M.; Li, F.; Han, T.; Yu, A.C.; Qin, P. Effects of ultrasound pulse parameters on cavitation properties of flowing microbubbles under physiologically relevant conditions. *Ultrason. Sonochem.* 2018, 52, 512–521.
23. Wang, M.; Zhang, Y.; Cai, C.; Tu, J.; Guo, X.; Zhang, D. Sonoporation-induced cell membrane permeabilization and cytoskeleton disassembly at varied acoustic and microbubble-cell parameters. *Sci. Rep.* 2018, 8, 1–12.
24. Kooiman, K.; Foppen-Harteveld, M.; van der Steen, A.F.; de Jong, N. Sonoporation of endothelial cells by vibrating targeted microbubbles. *J. Control. Release* 2011, 154, 35–41.
25. Supponen, O.; Akimura, T.; Minami, T.; Nakajima, T.; Uehara, S.; Ohtani, K.; Kaneko, T.; Farhat, M.; Sato, T. Jetting from cavitation bubbles due to multiple shockwaves. *Appl. Phys. Lett.* 2018, 113, 193703.
26. Fan, Z.; Chen, D.; Deng, C. Improving ultrasound gene transfection efficiency by controlling ultrasound excitation of microbubbles. *J. Control. Release* 2013, 170, 401–413.
27. Sojahrood, A.J.; de Leon, A.C.; Lee, R.; Cooley, M.; Abenojar, E.C.; Kolios, M.C.; Exner, A.A. Toward precisely controllable acoustic response of shell-stabilized nanobubbles: High yield and narrow dispersity. *ACS Nano* 2021, 15, 4901–4915.
28. Pellow, C.; Abenojar, E.C.; Exner, A.A.; Zheng, G.; Goertz, D.E. Concurrent visual and acoustic tracking of passive and active delivery of nanobubbles to tumors. *Theranostics* 2020, 10, 11690–11706.
29. Zhang, J.; Chen, Y.; Deng, C.; Zhang, L.; Sun, Z.; Wang, J.; Yang, Y.; Lv, Q.; Han, W.; Xie, M. The optimized fabrication of a novel nanobubble for tumor imaging. *Front. Pharmacol.* 2019, 10, 1–15.
30. Zheng, R.; Yin, T.; Wang, P.; Zheng, B.; Cheng, D.; Zhang, X.; Shuai, X.-T. Nanobubbles for enhanced ultrasound imaging of tumors. *Int. J. Nanomed.* 2012, 7, 895–904.
31. Rapoport, N.; Nam, K.-H.; Gupta, R.; Gao, Z.; Mohan, P.; Payne, A.; Todd, N.; Liu, X.; Kim, T.; Shea, J.; et al. Ultrasound-mediated tumor imaging and nanotherapy using drug loaded, block copolymer stabilized perfluorocarbon nanoemulsions. *J. Control. Release* 2011, 153, 4–15.

32. Versluis, M.; Stride, E.; Lajoinie, G.; Dollet, B.; Segers, T. Ultrasound contrast agent modeling: A review. *Ultrasound Med. Biol.* 2020, **46**, 2117–2144.

33. Komljenovic, D.; Bäuerle, T. Ultrasound imaging of cancer therapy. *Cancer Theranostics* 2014, 127–137.

34. Borden, M.A.; Pu, G.; Runner, G.J.; Longo, M.L. Surface phase behavior and microstructure of lipid/PEG-emulsifier monolayer-coated microbubbles. *Colloids Surf. B Biointerfaces* 2004, **35**, 209–223.

35. Amir, N.; Green, D.; Kent, J.; Xiang, Y.; Gorelikov, I.; Seo, M.; Blacker, M.; Janzen, N.; Czorny, S.; Valliant, J.F.; et al. ¹⁸F-Labeled perfluorocarbon droplets for positron emission tomography imaging. *Nucl. Med. Biol.* 2017, **54**, 27–33.

36. Williams, R.; Wright, C.; Cherin, E.; Reznik, N.; Lee, M.; Gorelikov, I.; Foster, F.S.; Matsuura, N.; Burns, P.N. Characterization of submicron phase-change perfluorocarbon droplets for extravascular ultrasound imaging of cancer. *Ultrasound Med. Biol.* 2013, **39**, 475–489.

37. Sheeran, P.S.; Matsuura, N.; Borden, M.A.; Williams, R.; Matsunaga, T.O.; Burns, P.N.; Dayton, P.A. Methods of generating submicrometer phase-shift perfluorocarbon droplets for applications in medical ultrasonography. *IEEE Trans. Ultrason. Ferroelectr. Freq. Control* 2016, **64**, 252–263.

38. Bloch, S.H.; Wan, M.; Dayton, P.A.; Ferrara, K.W. Optical observation of lipid- and polymer-shelled ultrasound microbubble contrast agents. *Appl. Phys. Lett.* 2004, **84**, 631–633.

39. Bouakaz, A.; Versluis, M.; de Jong, N. High-speed optical observations of contrast agent destruction. *Ultrasound Med. Biol.* 2005, **31**, 391–399.

40. Liu, Y.; Yan, J.; Prausnitz, M.R. Can ultrasound enable efficient intracellular uptake of molecules? A retrospective literature review and analysis. *Ultrasound Med. Biol.* 2012, **38**, 876–888.

41. Fateh, S.T.; Moradi, L.; Kohan, E.; Hamblin, M.R.; Dezfuli, A.S. Comprehensive review on ultrasound-responsive theranostic nanomaterials: Mechanisms, structures and medical applications. *Beilstein J. Nanotechnol.* 2021, **12**, 808–862.

42. Helfield, B.L.; Chen, X.; Qin, B.; Watkins, S.; Villanueva, F.S. Mechanistic insight into sonoporation with ultrasound-stimulated polymer microbubbles. *Ultrasound Med. Biol.* 2017, **43**, 2678–2689.

43. Shohet, R.V.; Chen, S.; Zhou, Y.-T.; Wang, Z.; Meidell, R.S.; Unger, R.H.; Grayburn, P.A. Echocardiographic destruction of albumin microbubbles directs gene delivery to the myocardium. *Circulation* 2000, **101**, 2554–2556.

44. Sirsi, S.; Borden, M.A. Microbubble compositions, properties and biomedical applications. *Bubble Sci. Eng. Technol.* 2009, **1**, 3–17.

45. Ferrara, K.; Borden, M.A.; Zhang, H. Lipid-shelled vehicles: Engineering for ultrasound molecular imaging and drug delivery. *Acc. Chem. Res.* 2009, 42, 881–892.
46. Piscaglia, F.; Bolondi, L. The safety of Sonovue in abdominal applications: Retrospective analysis of 23188 investigations. *Ultrasound Med. Biol.* 2006, 32, 1369–1375.

Retrieved from <https://encyclopedia.pub/entry/history/show/37386>